

# JOINTLY LEARNING VISUAL AND AUDITORY SPEECH REPRESENTATIONS FROM RAW DATA

Alexandros Haliassos<sup>1\*</sup> Pingchuan Ma<sup>1</sup> Rodrigo Mira<sup>1</sup> Stavros Petridis<sup>1,2</sup> Maja Pantic<sup>1,2</sup>

<sup>1</sup>Imperial College London

<sup>2</sup>Meta AI

alexandros.haliassos14@imperial.ac.uk

## ABSTRACT

We present RAVeN, a self-supervised multi-modal approach to jointly learn visual and auditory speech representations. Our pre-training objective involves encoding masked inputs, and then predicting contextualised targets generated by slowly-evolving momentum encoders. Driven by the inherent differences between video and audio, our design is *asymmetric* w.r.t. the two modalities’ pretext tasks: Whereas the auditory stream predicts both the visual and auditory targets, the visual one predicts only the auditory targets. We observe strong results in low- and high-resource labelled data settings when fine-tuning the visual and auditory encoders resulting from a *single* pre-training stage, in which the encoders are jointly trained. Notably, RAVeN surpasses all self-supervised methods on visual speech recognition (VSR) on LRS3, and combining RAVeN with self-training *using only 30 hours* of labelled data even outperforms a recent semi-supervised method trained on *90,000* hours of non-public data. At the same time, we achieve state-of-the-art results in the LRS3 low-resource setting for auditory speech recognition (as well as for VSR). Our findings point to the viability of learning powerful speech representations entirely from raw video and audio, *i.e.*, without relying on handcrafted features. Code and models will be made public.

## 1 INTRODUCTION

The sound of someone articulating words coincides with the sight of movements in and around their mouth. Both a recording of a speech waveform and a corresponding silent video of mouth motion provide rich - but not identical - information on which words were uttered. Despite the difficulty of interpreting lip movements compared with an audio waveform, the task of visual speech recognition (VSR; also known as lipreading) has important applications, ranging from recognising utterances in a noisy environment (Ma et al., 2021b; Afouras et al., 2018a; Martinez et al., 2020; Makino et al., 2019) and aiding people suffering from aphonia (an inability to speak), to transcribing archival silent films and detecting DeepFake videos (Haliassos et al., 2021).

Auditory (also known as automatic) speech recognition (ASR) and VSR benefit greatly from the combination of high-capacity neural networks and large datasets. Rapid advances of modern hardware are enabling the use of ever-growing, data-hungry networks, but the effort required for transcription hinders the scaling of labelled data along with the models. One way to leverage unlabelled videos for VSR is to use an external ASR model for pseudo-labelling (Afouras et al., 2020; Ma et al., 2022). However, this requires a large amount of labelled data to train a strong ASR model in the first place, and supervised VSR training with long sequences often poses optimisation problems, requiring costly curriculum learning strategies (Chung et al., 2017; Ma et al., 2022) or pre-training the feature extractor with isolated words (Afouras et al., 2018a; Ma et al., 2021b).

A solution is to first learn, in a self-supervised way, general representations from large corpora of unlabelled data, and then fine-tune them on smaller labelled datasets (Mohamed et al., 2022). The fine-grained correspondence between the (synchronised) visual and auditory modalities provides a natural source of self-supervision, and can produce highly semantic representations invariant to noise

---

\*Work done at Meta AI.

not shared between the modalities. However, approaches leveraging this correspondence either (1) only work for word-level samples rather than continuous speech (Chung & Zisserman, 2016; Chung et al., 2019; 2020); (2) use handcrafted features (e.g., spectrograms or MFCCs) as their inputs or targets (Ma et al., 2021a; Shi et al., 2022), which contain inductive biases that may influence the learned representations; (3) use multi-stage pre-training procedures (Ma et al., 2021a; Shi et al., 2022; Pan et al., 2022); and/or (4) use separate pre-training strategies for VSR and ASR (Shi et al., 2022), complicating the process of obtaining representations suitable for both tasks.

In this paper, we present a single-stage self-supervised approach that jointly learns visual and auditory speech representations from raw video and audio only. We dub our approach RAVeN (**R**aw **A**udio-**V**isual **S**peech **E**ncoders). It involves a pair of student-teacher networks for each modality, whereby the students encode temporally-masked inputs, and, through the use of lightweight Transformer-based predictors, regress outputs of momentum-based teachers (Grill et al., 2020; Caron et al., 2021) that are presented with unmasked inputs. Further, given that audio contains more information relevant to speech than video, we propose a learning strategy that accounts for the expected difference in the quality of targets between the modalities. Namely, while the audio student predicts outputs from both video and audio teachers (cross- and within-modal learning), the video student predicts only auditory targets (cross-modal learning). As we show, this setup leads to better downstream performance for both VSR and ASR as opposed to other strategies.

We conduct experiments with models and datasets of different sizes. We find that, when fine-tuning our pre-trained models for VSR and ASR with only 30 hours of labelled data from LRS3 (Afouras et al., 2018b), RAVeN surpasses recent self-supervised methods by a large margin in most settings. Coupling pre-training with self-training reaches 24.4% WER for VSR on LRS3, even outperforming a method trained on  $3000\times$  more transcribed hours (Serdyuk et al., 2021). At the same time, we are better than or on par with the recent AV-HuBERT method (Shi et al., 2022) on ASR, without using a task-dependent pre-training strategy nor handcrafted features. Using the full 433-hour LRS3 dataset for fine-tuning pushes the results even further, achieving 23.4% / 1.4% WER for VSR / ASR, respectively. Similarly strong performance is observed on the LRS2 dataset (Appendix B).

## 2 RELATED WORK

**Masked prediction.** The pre-training task of predicting missing content given masked inputs has proven successful in various domains, such as natural language processing (Devlin et al., 2019; Radford et al., 2018; 2019; Brown et al., 2020), image recognition (He et al., 2021; Xie et al., 2022; Bao et al., 2021), and speech recognition (Baevski et al., 2020; Hsu et al., 2021; Shi et al., 2022). An important aspect of masked prediction is the nature of the targets. Some works (He et al., 2021; Xie et al., 2022) use pixels as targets; others use pre-trained tokenisers (Bao et al., 2021) or modality-specific handcrafted features (Wei et al., 2021; Hsu et al., 2021; Shi et al., 2022). Our method, in contrast, generates targets from *raw video and audio* using momentum encoders.

**Self-distillation for unsupervised representation learning.** RAVeN is partly inspired by the success of self-distillation in self-supervised learning with visual data (Grill et al., 2020; Caron et al., 2021); such works target invariance w.r.t. image-specific augmentations. In contrast, RAVeN does not rely on domain-specific augmentations but rather on a combination of cross-modal learning and masked prediction to drive representation learning for visual and auditory speech signals. data2vec (Baevski et al., 2022) combines masked prediction with a momentum encoder, but, aside from being uni-modal, it is different methodologically in multiple ways. For example, it applies ad-hoc normalisation and averaging techniques to the targets to prevent representation collapse, while our targets are simply the outputs of the encoders, which are regressed via Transformer-based heads.

**Self-supervised audiovisual learning.** Audiovisual correspondence has been used to learn global representations for action recognition through the use of clustering (Alwassel et al., 2020; Asano et al., 2020), contrastive learning (Arandjelovic & Zisserman, 2017; 2018; Korbar et al., 2018; Patrick et al., 2020; Morgado et al., 2021; Ma et al., 2021c), or representation matching (Recasens et al., 2021). Cross-modal learning has also found uses in biometric matching (Nagrani et al., 2018a;b), emotion recognition (Shukla et al., 2021), and DeepFake detection (Haliassos et al., 2022). We employ cross- and within-modal losses to learn temporally-varying speech representations.

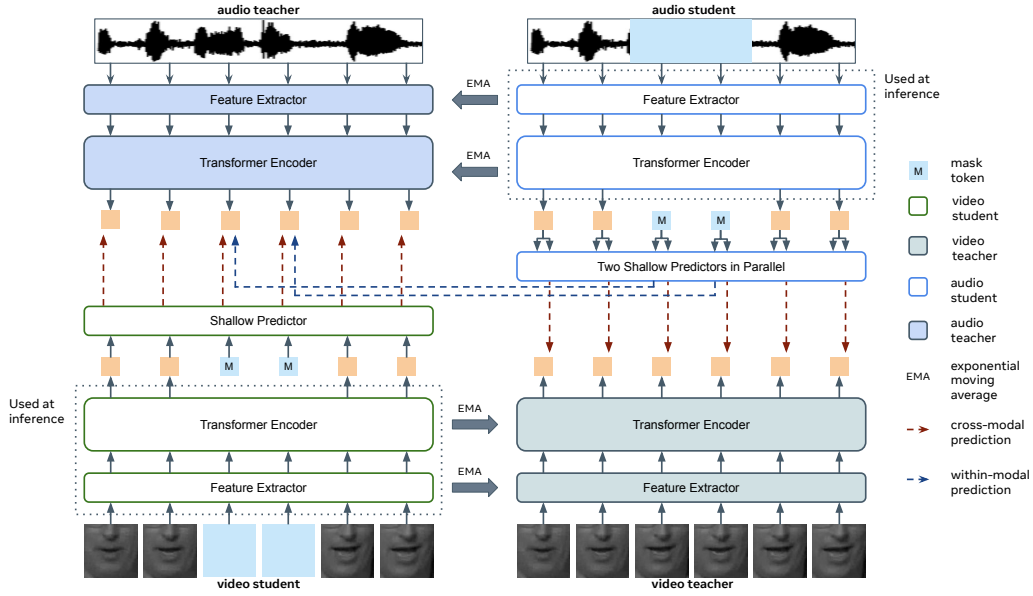


Figure 1: **RAVeN overview.** Given masked video and audio, students predict outputs of momentum teachers, via shallow Transformer predictors that intake mask tokens. Teacher inputs are not masked. The audio student predicts outputs from both audio and video teachers, whereas the video student predicts only audio targets. Cross-modal losses are applied on all features; the within-modal loss is computed only on masked features. Only the student encoders are fine-tuned for VSR/ASR.

**Self-supervised audiovisual learning for speech recognition.** Earlier audiovisual self-supervised works (Chung & Zisserman, 2016; Chung et al., 2019; 2020) tended to focus on word-level lipreading. Recently, some attention has been paid to the more realistic task of *continuous* speech recognition (Ma et al., 2021a; Shi et al., 2022; Sheng et al., 2021; Pan et al., 2022; Ma et al., 2021c). Sheng et al. (2021); Ma et al. (2021c) use contrastive learning and apply their method to VSR. Ma et al. (2021a) predict speech features using an external PASE+ encoder (Ravanelli et al., 2020). Pan et al. (2022) transfer pre-trained visual and auditory encoders, which were separately trained via contrastive losses. AV-HuBERT (Shi et al., 2022) predicts iteratively-refined cluster assignments from masked audiovisual inputs and achieves impressive VSR and ASR performance. It employs multiple stages of alternating between offline clustering and cluster assignment prediction, and relies on hand-crafted audio features (MFCCs) for cluster initialisation, which is shown to be crucial to the performance (Shi et al., 2022). We demonstrate that it is possible to jointly learn effective representations for VSR and ASR in a single stage simply from raw video and audio.

### 3 METHOD

#### 3.1 PRE-TRAINING

Our architecture consists of a pair of student-teacher networks per modality (see Figure 1). The students intake masked inputs and predict targets formed by teachers receiving unmasked inputs.

**Masking.** We employ masking to encourage the students to take context into account when solving the task. Given a grayscale video  $x^v \in \mathbb{R}^{T \times H \times W}$  with resolution  $(H, W)$  and  $T$  frames, and an audio sample  $x^a \in \mathbb{R}^N$  of length  $N$ , we randomly sample with probability 0.2 each video frame to be the starting mask index, and if selected, then the consecutive three frames are zeroed out (ablation in Section 4.4). A similar mask is applied to the auditory input, except that it is enlarged by a factor of  $16\,000/25 = 640$  (since the audio is sampled at 16,000 Hz and the video at 25 fps).

**Encoders.** The masked video and audio,  $\bar{x}^v$  and  $\bar{x}^a$  respectively, are fed to their corresponding student encoders  $f_e^v$  and  $f_e^a$ , yielding features  $f_e^v(\bar{x}^v) \in \mathbb{R}^{T \times D}$  and  $f_e^a(\bar{x}^a) \in \mathbb{R}^{T \times D}$ , where  $D$  is

the dimensionality of each feature. Both  $f_e^v$  and  $f_e^a$  consist of a modality-specific, convolutional feature extractor followed by a temporal encoder, as in related VSR/ASR works (Ma et al., 2022; Baeviski et al., 2020). The video feature extractor is a 2D ResNet18 (He et al., 2016) with a 3D convolutional stem (Petridis et al., 2018), outputting an embedding per frame. On the audio side, we use a 1D ResNet18 which produces features at 25 fps, to match the video sampling rate (see Appendix A.5). The temporal encoder for each modality is a Transformer (Vaswani et al., 2017) (without a classification head) with hidden size  $D$ . We use relative positional embeddings (Dai et al., 2019), and following Chen et al. (2021), we replace layernorm (Ba et al., 2016) with batchnorm (Ioffe & Szegedy, 2015) before each multilayer perceptron (MLP) block (see Appendix C.1 for a comparison).

**Predictors.** The students contain Transformer predictors, which regress targets given 1) the encoder outputs corresponding to the unmasked portions of the inputs and 2) mask tokens associated with the masked portions. Note that mask tokens are applied to the predictors rather than the encoders (He et al., 2021). This reduces the discrepancy between pre-training and fine-tuning: In both cases, the encoders do not see mask tokens. A predictor that takes representations corresponding to modality  $m_1 \in \{v, a\}$  and predicts targets associated with modality  $m_2 \in \{v, a\}$  is denoted as  $f_p^{m_1 \rightarrow m_2}$ . For ease, the application of mask tokens to the encoder outputs is absorbed in the notation.

Unlike other works which output global representations (one embedding per sample) and thus use MLPs as predictors (Grill et al., 2020; Chen et al., 2021), we use Transformers to allow modelling temporal dynamics, which we found greatly improves results. The predictors can be lightweight: Indeed, two-block Transformers with hidden size 512 work optimally in our experiments.

**Targets.** The targets are simply the outputs of momentum-based teachers  $g^v$  and  $g^a$  (Grill et al., 2020; Caron et al., 2021), which are given as input the unmasked video or audio, in order to force the students to predict the missing information. Each teacher is architecturally identical to its student encoder counterpart. Denoting the parameters of the student encoders and teachers as  $s^m$  and  $t^m$ , respectively, at each iteration the following update is performed:

$$t^m \leftarrow \mu t^m + (1 - \mu) s^m, \quad (1)$$

where  $m \in \{v, a\}$  specifies the modality and  $\mu$  is a momentum parameter following a cosine schedule from 0.999 to 1. A high value of  $\mu$  leads to slowly-varying teachers and stable targets. The use of momentum-based teachers obviates the need for handcrafted targets or multi-stage training.

**Prediction tasks.** The auditory modality contains more information relevant to speech than the visual one: Mouth motion is inherently more ambiguous than a speech waveform due to the presence of homophemes (Chung et al., 2017). We propose a loss structure which reflects this asymmetry between the modalities. The audio student predicts the targets from both the video and audio teacher, thus benefiting from the ability of cross-modal learning to induce semantic representations, while at the same time being encouraged to retain information from the auditory input that is absent from the visual one. As a result, two predictors are associated with the audio student, one for each target type. On the other hand, the video student only predicts the auditory targets, which are inevitably of higher quality.

**Losses.** The loss function is the negative cosine similarity (Grill et al., 2020), denoted as  $\text{sim}$ . Due to the temporal alignment of the inputs, the cosine similarity is applied between pairs of corresponding features and then summed across the time dimension. For the within-modal task (audio-to-audio prediction), the loss is applied only on targets corresponding to masked portions of the input (Devlin et al., 2019). For the cross-modal tasks, the loss is applied on all targets, which we found to work better. Note that predicting the unmasked portions in cross-modal learning is a non-trivial task (unlike in within-modal learning) and can bolster representation learning.

Denoting the set of mask token indices for audio as  $M_a$ , the audio-to-audio prediction loss and cross-modal losses can be respectively expressed as

$$\mathcal{L}^{a \rightarrow a} = - \sum_{n \in M_a} \text{sim} \left( f_p^{a \rightarrow a} \left( f_e^a (\bar{x}^a) \right)_n, \text{sg} \left( g^a (x^a)_n \right) \right), \quad (2)$$

$$\mathcal{L}^{m_1 \rightarrow m_2} = - \sum_n \text{sim} \left( f_p^{m_1 \rightarrow m_2} \left( f_e^{m_1} (\bar{x}^{m_1}) \right)_n, \text{sg} \left( g^{m_2} (x^{m_2})_n \right) \right), \quad (3)$$

where  $m_1, m_2 \in \{v, a\}$ ,  $m_1 \neq m_2$ , and  $\text{sg}$  denotes the “stop-gradient” operation, which indicates that no gradient is passed back to the teacher networks..

**Objectives.** At each iteration, the objectives for the video and audio students are, respectively,

$$\mathcal{L}_v = \mathcal{L}^{v \rightarrow a}, \quad \mathcal{L}_a = \mathcal{L}^{a \rightarrow v} + \mathcal{L}^{a \rightarrow a}. \quad (4)$$

The teachers are updated via Equation 1.

### 3.2 FINE-TUNING

For fine-tuning, we keep the pre-trained student encoders and discard the rest. We append a linear layer and a Transformer decoder for joint CTC / attention decoding (Watanabe et al., 2017), as in Ma et al. (2021b). Following Ma et al. (2021b), we set the CTC weight to 0.1. We use SentencePiece (Kudo & Richardson, 2018) subword units with a vocabulary size of 1,000 as our targets.

**Self-training.** Combining pre-training with self-training tends to improve results over using either strategy in isolation (Xu et al., 2021; Shi et al., 2022). To that end, we first fine-tune our pre-trained audio encoder on the labelled data, and then use the model for pseudo-labelling the unlabelled data. The pre-trained video and audio models are then fine-tuned using both the labels and pseudo-labels.

## 4 EXPERIMENTS

### 4.1 SETUP

**Datasets.** For pre-training, we conduct experiments with LRS3 (Afouras et al., 2018b) (without the labels) as well as a combination of LRS3 and an English-only version of VoxCeleb2 (Chung et al., 2018) curated by Shi et al. (2022), which we refer to as LRS3+Vox2-en. The former features 433 hours of footage and the latter 1,759 hours. For fine-tuning, we use the full LRS3 with the labels as our high-resource labelled data setting, as well as a 30-hour subset (the “trainval” partition) as our low-resource setting. We present results for the LRS2 dataset (Chung et al., 2017) in Appendix B.

**Transformer encoder.** We show results for two configurations of the Transformer encoders, Base and Large, with 12 and 24 blocks respectively. The hidden size/MLP size/attention heads are 512/2048/8 for Base and 1024/4096/16 for Large, amounting to 41 million (M) and 328 M parameters, respectively. We note that our Base model is around half the size of the one used by Shi et al. (2022) and the Large models are similar in size. Training details are provided in Appendix A.

### 4.2 LOW-RESOURCE LABELLED DATA SETTING

We pre-train our models on LRS3 and/or LRS3+Vox2-en and then fine-tune them on the 30-hour LRS3 subset to evaluate performance when labels are scarce. We reports results in Table 1.

Compared with training from scratch, RAVen pre-training leads to dramatic performance improvements in all configurations. Notably, increasing the model size *hurts* VSR performance when training from scratch, but *improves* it when using pre-training.

Our Base variant outperforms all related methods on VSR. It surpasses the Base AV-HuBERT model by 4.8% and 5.9% WER when using LRS3 and LRS3+Vox2-en, respectively, despite having roughly half the number of parameters. The Large model provides significant boosts over the Base model (33.1% vs 40.2% WER) when using LRS3+Vox2-en for pre-training, keeping the number of labelled data points fixed. Self-training further improves WER by 6.9%, indicating its complementarity with RAVen pre-training. Finally, using a language model (see Appendix A.4 for details) leads to a WER of 24.4%, better than a method (Serdyuk et al., 2021) trained on 90,000 hours of non-public data.

On ASR, RAVen significantly outperforms the audio-only Hubert (Hsu et al., 2021) model, and in all cases is better than or on par with AV-HuBERT. Our best ASR model without self-training achieves 2.6% WER vs AV-HuBERT’s 2.9% WER, despite AV-HuBERT using a different pre-training strategy for VSR than ASR. For example, using the same pre-training hyperparameters increases AV-HuBERT’s WER for ASR from 3.8% to 4.6% with the Base model (Shi et al., 2022). In contrast,

Method	Encoder	LM	Unlab hours	Lab hours	WER (%)	
					VSR	ASR
supervised						
Afouras et al. (2018a)	Transformer	✓	-	1,519*	58.9	8.3
Xu et al. (2020)	RNN	✗	-	590	57.8	7.2
Shillingford et al. (2019)	RNN	✓	-	3,886*	55.1	-
Ma et al. (2022)	Conformer	✓	-	813	34.7	-
Makino et al. (2019)	RNN	✗	-	31,000*	33.6	4.8
Prajwal et al. (2022)	Transformer	✓	-	2,676*	30.7	-
Serdyuk et al. (2021)	Transformer	✗	-	90,000*	25.9	2.3
Serdyuk et al. (2022)	Conformer	✗	-	90,000*	19.3	1.6
from scratch						
Base model	Transformer	✗	-	30	93.4	18.5
Large model	Transformer	✗	-	30	95.5	9.9
self-supervised						
Base models, less pre-training data						
Ma et al. (2021a)	Transformer	✗	433	30	71.9 <sup>†</sup>	-
Zhang et al. (2022)	Transformer	✗	433	30	67.8	10.9
Hsu et al. (2021)	Transformer	✗	433	30	-	5.4
Shi et al. (2022)	Transformer	✗	433	30	51.8	4.9
RAVEN	Transformer	✗	433	30	47.0	4.7
Base models, more pre-training data						
Hsu et al. (2021)	Transformer	✗	1,759	30	-	5.0
Shi et al. (2022)	Transformer	✗	1,759	30	46.1	4.6 <sup>‡</sup> / 3.8
RAVEN	Transformer	✗	1,759	30	40.2	3.8
Large models, more pre-training data						
Hsu et al. (2021)	Transformer	✗	1,759	30	-	3.2
Shi et al. (2022)	Transformer	✗	1,759	30	32.5	2.9
Shi et al. (2022) w/ self-training	Transformer	✗	1,759	30	28.6	-
RAVEN	Transformer	✗	1,759	30	33.1	2.6
RAVEN w/ self-training	Transformer	✗	1,759	30	26.2	2.2
RAVEN w/ self-training	Transformer	✓	1,759	30	24.4	1.9

Table 1: **LRS3 low-resource setting.** We report results on the test set when fine-tuning on 30 hours of LRS3 with different model sizes and number of unlabelled data hours (Unlab hours). LM denotes whether or not a language model was used during decoding. We also provide baselines for training our models from scratch (without our pre-training) and results from supervised methods trained on more labelled data hours (Lab hours) for reference. \*Includes non-publicly available data, some of which is not hand-labelled. <sup>†</sup>Result taken from Shi et al. (2022). <sup>‡</sup>Result with the same pre-training strategy for VSR and ASR.

the video and audio encoders we use for fine-tuning are the result of a *single* pre-training phase, where they were jointly learned.

All in all, our results suggest that transcribed data, which are costly to obtain, can be largely substituted with raw unlabelled audiovisual data.

### 4.3 HIGH-RESOURCE LABELLED DATA SETTING

Table 2 reports results when fine-tuning on the full 433 hours of LRS3. Despite increasing the labelled data, training the model *from scratch* still leads to poor performance, as in the low-resource setting. This is likely related to the long utterances in the LRS3 dataset, which may cause optimisation difficulties (Ma et al., 2022). A potential remedy is to employ curriculum learning, as proposed by Ma et al. (2022), by training the network in multiple stages with increasingly longer sequences. We observe that this strategy indeed reduces WER from 87.3% to 39.8% for the Base model. Even so, pre-training with the same data used for fine-tuning leads to a better WER of 39.1%, *without* requiring a curriculum learning procedure. This suggests that self-supervised pre-training can aid optimisability. The impact of pre-training is even more pronounced with the Large model.

Method	Encoder	LM	Unlab hours	Lab hours	WER (%)	
					VSR	ASR
<i>semi-supervised (using external models for pseudo-labelling)</i>						
Afouras et al. (2020)	CNN	✓	344	433	59.8	-
Ma et al. (2022)	Conformer	✓	641	818	<b>31.5</b>	-
<i>from scratch</i>						
Base model	Transformer	✗	-	433	87.3	2.5
Base model w/ curriculum	Transformer	✗	-	433	39.8	-
Large model	Transformer	✗	-	433	85.8	<b>2.2</b>
Large model w/ curriculum	Transformer	✗	-	433	<b>38.8</b>	-
<i>self-supervised</i>						
<b>Base models, less pre-training data</b>						
Shi et al. (2022)	Transformer	✗	433	433	44.0	-
RAVEN	Transformer	✗	433	433	<b>39.1</b>	<b>2.2</b>
<b>Base models, more pre-training data</b>						
Ma et al. (2021a)	Transformer	✗	1,759	433	49.6 <sup>†</sup>	-
Hsu et al. (2021)	Transformer	✗	1,759	433	-	2.4
Shi et al. (2022)	Transformer	✗	1,759	433	34.8	2.0
RAVEN	Transformer	✗	1,759	433	<b>33.1</b>	<b>1.9</b>
<b>Large models, more pre-training data</b>						
Hsu et al. (2021)	Transformer	✗	1,759	433	-	1.5
Shi et al. (2022)	Transformer	✗	1,759	433	28.6	<b>1.3</b>
Shi et al. (2022) w/ self-training	Transformer	✗	1,759	433	26.9	-
RAVEN	Transformer	✗	1,759	433	28.2	1.4
RAVEN w/ self-training	Transformer	✗	1,759	433	24.9	1.4
RAVEN w/ self-training	Transformer	✓	1,759	433	<b>23.4</b>	1.4

Table 2: **LRS3 high-resource setting.** We report results on the test set with different model sizes and number of unlabelled data hours (Unlab hours). Lab hours denotes the number of labelled hours, and LM denotes whether or not a language model was used during decoding. We provide baselines for training our models from scratch (without our pre-training). <sup>†</sup>Result taken from Shi et al. (2022).

RAVEN outperforms AV-HuBERT under all configurations on VSR. Our best result is 23.4%, achieved using self-training and a language model. We note that unlike methods that use external ASR models (Afouras et al., 2020; Ma et al., 2022) for pseudo-labelling, we do not require extra data for the self-training phase.

We are on par with the state-of-the-art for ASR in the high-resource setting, achieving a WER of 1.4% with the Large model. This is despite using raw audio as input (rather than spectrograms which Shi et al. (2022) use). We notice that additionally including self-training and a language model does not reduce the WER, suggesting that the ASR performance may have saturated in our environment.

#### 4.4 PRE-TRAINING ABLATIONS

Ablations are performed with our Base model in the low-resource setting with LRS3 pre-training using the validation set from Shi et al. (2022) (as there is no official development set). For more ablations, see Appendix C.

**Prediction tasks.** We study in Table 3 the impact of cross- and within-modal prediction on the learned representations. Figure 2 illustrates the various prediction tasks we consider. We observe the following. The *within-modal* variant performs decently for ASR but poorly for VSR, which can be explained by the assumption that audio contains more speech information than video. The *cross-modal* variant performs better than within-modal for both modalities. Since lip movements and the corresponding waveform are correlated in terms of lexical content, the representations resulting from cross-modal prediction are expected to capture rich semantic information. At the same time, they are likely to be, to a large extent, invariant to factors unshared between the two modalities, such as visual or auditory noise, benefiting generalisation. Combining *cross- with within-modal*

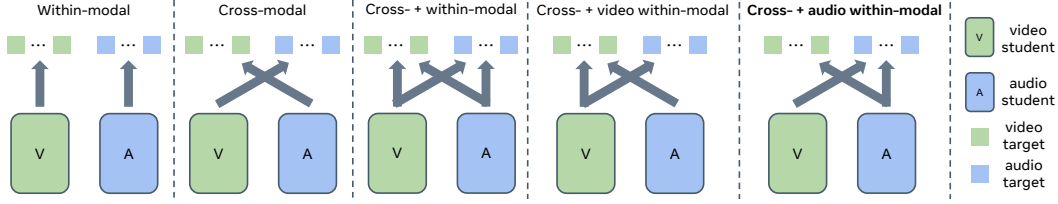


Figure 2: **Prediction tasks.** We consider different choices for our prediction tasks, combining cross- and within-modal losses. We find that applying both cross- and within-modal losses for the audio student, and only a cross-modal loss for the video student works best.

Setting	Prediction tasks				WER (%)	
	V $\rightarrow$ V	A $\rightarrow$ A	V $\rightarrow$ A	A $\rightarrow$ V	VSR	ASR
Within-modal	✓	✓	✗	✗	92.7	15.5
Cross-modal	✗	✗	✓	✓	40.8	14.0
Cross- + within-modal	✓	✓	✓	✓	49.0	14.0
Cross- + video within-modal	✓	✗	✓	✓	55.3	16.4
Cross- + audio within-modal	✗	✓	✓	✓	<b>32.9</b>	<b>12.2</b>

Table 3: **Prediction task** ablations under the LRS3 low-resource setting using our Base model. V  $\rightarrow$  A means that the video student predicts the audio teacher representations. Each prediction loss is associated with a separate predictor.

learning hurts VSR relative to only cross-modal prediction. However, cross-modal with within-modal learning *only for audio* achieves the best results. We hypothesise that predicting the auditory targets forces the auditory stream to keep relevant information absent from the visual stream. We note that removing the video-to-video prediction (from row 3 to row 5 in Table 3) also improves the audio student, as the quality of the visual targets improves. Finally, cross-modal with within-modal learning *only for video* does not perform well, validating that the asymmetry only works one way.

**Masking sampling.** Table 4a studies the effect of different masking strengths by varying the mask length and probability that a given index is chosen as the mask start. We observe that a probability of 0.2 and a length of three video frames (corresponding to 1,920 audio samples) works well. Less masking allows the student to focus less on context and degrades both VSR and ASR. Interestingly, although more masking hurts VSR, it helps ASR, suggesting that an asymmetric masking strategy w.r.t. the two modalities may further improve results. We leave this exploration to future work.

Our masking is less aggressive than what was found to be optimal in related self-supervised image and action recognition literature (where 75% or even 90% of the input is masked) (He et al., 2021; Tong et al., 2022). We hypothesise that mouth movements are fast-varying and do not contain much temporal redundancy, and thus such strong masking makes our pretext task overly difficult.

Prob	Length	WER (%)	
		VSR	ASR
0.1	1	41.1	15.6
0.2	3	<b>32.9</b>	12.2
0.4	5	35.7	<b>11.7</b>

Position	WER (%)	
	VSR	ASR
Encoder	43.1	14.0
Predictor	<b>32.9</b>	<b>12.2</b>

Loss	WER (%)	
	VSR	ASR
Masked	44.3	12.6
All	<b>32.9</b>	<b>12.2</b>

(a) **Masking strength** in terms of starting index probability and mask length.

(b) **Mask token position.** Applying the mask tokens in the predictor works better than in the encoder.  
(c) **Cross-modal loss.** Applying the cross-modal loss for all inputs is superior to applying it only for masked inputs.

Table 4: **Masking** ablations under the LRS3 low-resource setting using our Base model.

Predictor type	Params	WER (%)	
		VSR	ASR
None	0	coll. <sup>‡</sup>	coll. <sup>‡</sup>
Linear	0.3M	64.4	17.7
MLP	4.2M	62.6	19.0
Transformer 1 block	3.9M	46.7	14.1
Transformer 2 blocks	7.4M	<b>32.9</b>	<b>12.2</b>
Transformer 4 blocks	14.2M	46.2	13.4

(a) **Predictor type.** A lightweight Transformer predictor works better than a linear layer or 2-layer MLP design. <sup>‡</sup>Denotes representation collapse.

Att dim	MLP dim	WER (%)	
		VSR	ASR
256	1024	44.0	13.3
512	2048	<b>32.9</b>	<b>12.2</b>
1024	4096	39.1	12.3

(b) **Predictor width.** A moderate predictor width works optimally.

Table 5: **Predictor capacity** ablations under the LRS3 low-resource setting using our Base model.

**Mask token position.** We investigate in Table 4b the optimal position of the mask tokens. It is clear that better performance is achieved when applying them in the predictors rather than the encoders. Forgoing the use of mask tokens in the encoders leads to no input discrepancy between pre-training and fine-tuning, since no mask tokens are used during fine-tuning.

**Mask loss.** It is common to apply the loss only on masked inputs for *within-modal* losses (Hsu et al., 2021; He et al., 2021), since predicting targets corresponding to unmasked inputs may be trivial. However, this is not the case for cross-modal prediction, where the targets are not related to the inputs in an obvious way. Indeed, Table 4c shows that applying the loss for both masked and unmasked inputs outperforms applying it only for masked inputs.

**Predictor design.** Table 5a shows the effect of different predictor types. We note that using no predictors at all leads to representation collapse, where all outputs are constant (Grill et al., 2020). We compare linear layers and 2-layer MLPs (applied independently to each encoder output) with Transformers of varying capacity. Following Grill et al. (2020), the MLPs have hidden dimension of 4096 with batchnorm followed by ReLU (Nair & Hinton, 2010) after the hidden layer.

We find that a Transformer predictor works significantly better, even when the number of parameters in the (1-block) Transformer and the 2-layer MLP is similar. Interestingly, the ability for the predictors to model temporal dependencies seems to be crucial to our representation learning phase.

A two-block Transformer works optimally (Table 5a). A shallower Transformer likely results in representations too specialised to the pretext task. A deeper one might place a lot of the burden on the predictors, leaving the encoder representations too general. Similar conclusions can be drawn regarding the Transformer width (see Table 5b). Overall, the lightweight predictor design means that using three predictors (one on the video student side and two on the audio) has relatively little effect on the total computational cost.

## 5 CONCLUSION

We presented RAVEn, a single-stage method that jointly learns visual and auditory speech representations entirely from raw data. It employs momentum encoders to generate targets, which, given masked inputs, are predicted by Transformer encoders and predictors. Especially salient to the quality of the representations are appropriate masking, lightweight Transformer predictors, and an asymmetric loss structure w.r.t. the visual and auditory modalities. RAVEn achieves strong performance under many settings without requiring multiple pre-training stages, handcrafted audio targets, or separate pre-training strategies for VSR and ASR.

As future work, it would be interesting to examine the effect of sharing weights between the visual and auditory encoders as a way of reducing the memory requirements for pre-training. We would also like to apply RAVEn to other tasks related to speech. We hope our study inspires future research extending beyond speech recognition.

---

## ETHICS STATEMENT

Despite numerous positive applications, our method can also be misused. For example, lipreading technologies can be employed for surveillance, compromising the public’s privacy and trust. This problem is likely to be exacerbated as the quality of CCTV cameras improves over time. Appropriate government regulations will need to be put in place to limit such concerns. Another issue relates to the potential biases embedded in the datasets used. Such biases may have to do with gender, age, or ethnic backgrounds. A specific group being under-represented in the data would likely result in reduced model performance on samples belonging to said group. Making sure that the models are trained on balanced data, or using other bias-reduction techniques, can address such issues.

Our work used datasets that were made public for research purposes, i.e., LRS2, LRS3, and Vox-Celeb2. In particular, we used the cropped face .mp4 videos that were available on the official dataset webpages and which complied with the following licenses: Creative Commons BY-NC-ND 4.0 license and Creative Commons Attribution 4.0 International License, TED terms of use, and BBC’s terms of use.

## REPRODUCIBILITY

To ensure reproducibility, we provide as many implementation details as possible in the main paper as well as tables showing the hyperparameter values in the appendix. Moreover, we plan on making the code and pre-trained models publicly available.

## ACKNOWLEDGEMENTS

Only non-Meta co-authors downloaded, accessed, and used the LRS2 dataset.

## REFERENCES

- Triantafyllos Afouras, Joon Son Chung, Andrew Senior, Oriol Vinyals, and Andrew Zisserman. Deep audio-visual speech recognition. *IEEE Transactions on Pattern Analysis and Machine Intelligence*, 2018a.
- Triantafyllos Afouras, Joon Son Chung, and Andrew Zisserman. LRS3-TED: a large-scale dataset for visual speech recognition. *arXiv preprint arXiv:1809.00496*, 2018b.
- Triantafyllos Afouras, Joon Son Chung, and Andrew Zisserman. Asr is all you need: Cross-modal distillation for lip reading. In *Proceedings of the 45th IEEE International Conference on Acoustics, Speech and Signal Processing (ICASSP)*, pp. 2143–2147, 2020.
- Humam Alwassel, Dhruv Mahajan, Bruno Korbar, Lorenzo Torresani, Bernard Ghanem, and Du Tran. Self-supervised learning by cross-modal audio-video clustering. *Proceedings of the 33rd Advances in Neural Information Processing System (NIPS)*, 33:9758–9770, 2020.
- Relja Arandjelovic and Andrew Zisserman. Look, listen and learn. In *Proceedings of the 16th IEEE/CVF International Conference on Computer Vision (ICCV)*, pp. 609–617, 2017.
- Relja Arandjelovic and Andrew Zisserman. Objects that sound. In *Proceedings of the 15th European Conference on Computer Vision (ECCV)*, pp. 435–451, 2018.
- Rosana Ardila, Megan Branson, Kelly Davis, Michael Kohler, Josh Meyer, Michael Henretty, Reuben Morais, Lindsay Saunders, Francis M. Tyers, and Gregor Weber. Common voice: A massively-multilingual speech corpus. In *Proceedings of the 12th Language Resources and Evaluation Conference*, pp. 4218–4222, 2020.
- Yuki Asano, Mandela Patrick, Christian Rupprecht, and Andrea Vedaldi. Labelling unlabelled videos from scratch with multi-modal self-supervision. *Proceedings of the 33rd Advances in Neural Information Processing System (NIPS)*, 33:4660–4671, 2020.

- 
- Jimmy Lei Ba, Jamie Ryan Kiros, and Geoffrey E Hinton. Layer normalization. *arXiv preprint arXiv:1607.06450*, 2016.
- Alexei Baevski, Yuhao Zhou, Abdelrahman Mohamed, and Michael Auli. wav2vec 2.0: A framework for self-supervised learning of speech representations. In *Proceedings of the 33rd Advances in Neural Information Processing System (NIPS)*, volume 33, pp. 12449–12460, 2020.
- Alexei Baevski, Wei-Ning Hsu, Qiantong Xu, Arun Babu, Jiatao Gu, and Michael Auli. Data2vec: A general framework for self-supervised learning in speech, vision and language. *arXiv preprint arXiv:2202.03555*, 2022.
- Hangbo Bao, Li Dong, and Furu Wei. Beit: Bert pre-training of image transformers. *arXiv preprint arXiv:2106.08254*, 2021.
- Tom Brown, Benjamin Mann, Nick Ryder, Melanie Subbiah, Jared D Kaplan, Prafulla Dhariwal, Arvind Neelakantan, Pranav Shyam, Girish Sastry, Amanda Askell, et al. Language models are few-shot learners. *Proceedings of the 33rd Advances in Neural Information Processing System (NIPS)*, 33:1877–1901, 2020.
- Adrian Bulat and Georgios Tzimiropoulos. How far are we from solving the 2d & 3d face alignment problem?(and a dataset of 230,000 3d facial landmarks). In *Proceedings of the 16th IEEE/CVF International Conference on Computer Vision (ICCV)*, pp. 1021–1030, 2017.
- Mathilde Caron, Hugo Touvron, Ishan Misra, Hervé Jégou, Julien Mairal, Piotr Bojanowski, and Armand Joulin. Emerging properties in self-supervised vision transformers. In *Proceedings of the 18th IEEE/CVF International Conference on Computer Vision (ICCV)*, pp. 9650–9660, 2021.
- Xinlei Chen, Saining Xie, and Kaiming He. An empirical study of training self-supervised vision transformers. In *Proceedings of the 18th IEEE/CVF International Conference on Computer Vision (ICCV)*, pp. 9640–9649, 2021.
- Joon Son Chung and Andrew Zisserman. Out of time: automated lip sync in the wild. In *Proceedings of the 13th Asian Conference on Computer Vision (ACCV)*, pp. 251–263, 2016.
- Joon Son Chung, Andrew Senior, Oriol Vinyals, and Andrew Zisserman. Lip reading sentences in the wild. In *Proceedings of the 30th IEEE/CVF Conference on Computer Vision and Pattern Recognition (CVPR)*, pp. 3444–3453, 2017.
- Joon Son Chung, Arsha Nagrani, and Andrew Zisserman. Voxceleb2: Deep speaker recognition. In *Proceedings of the 19th Annual Conference of International Speech Communication Association (INTERSPEECH)*, pp. 1086–1090, 2018.
- S. Chung, J. Son Chung, and H. Kang. Perfect match: Improved cross-modal embeddings for audio-visual synchronisation. In *Proceedings of the 44th IEEE International Conference on Acoustics, Speech and Signal Processing (ICASSP)*, pp. 3965–3969, 2019.
- Soo-Whan Chung, Hong-Goo Kang, and Joon Son Chung. Seeing voices and hearing voices: learning discriminative embeddings using cross-modal self-supervision. In *Proceedings of the 21st Annual Conference of International Speech Communication Association (INTERSPEECH)*, pp. 3486–3490, 2020.
- Kevin Clark, Minh-Thang Luong, Quoc V Le, and Christopher D Manning. ELECTRA: pre-training text encoders as discriminators rather than generators. In *Proceedings of the 8th International Conference on Learning Representations (ICLR)*, 2020.
- Zihang Dai, Zhilin Yang, Yiming Yang, Jaime G. Carbonell, Quoc Viet Le, and Ruslan Salakhutdinov. Transformer-xl: Attentive language models beyond a fixed-length context. In *Proceedings of the 57th Conference of the Association for Computational Linguistics (ACL)*, pp. 2978–2988, 2019.
- Jiankang Deng, Jia Guo, Evangelos Ververas, Irene Kotsia, and Stefanos Zafeiriou. Retinaface: Single-shot multi-level face localisation in the wild. In *Proceedings of the 33rd IEEE/CVF Conference on Computer Vision and Pattern Recognition (CVPR)*, pp. 5203–5212, 2020.

- 
- Jacob Devlin, Ming-Wei Chang, Kenton Lee, and Kristina Toutanova. BERT: pre-training of deep bidirectional transformers for language understanding. In *Proceedings of the Conference of the North American Chapter of the Association for Computational Linguistics: Human Language Technologies, NAACL-HLT*, pp. 4171–4186, 2019.
- Priya Goyal, Piotr Dollár, Ross Girshick, Pieter Noordhuis, Lukasz Wesolowski, Aapo Kyrola, Andrew Tulloch, Yangqing Jia, and Kaiming He. Accurate, large minibatch sgd: Training imagenet in 1 hour. *arXiv preprint arXiv:1706.02677*, 2017.
- Jean-Bastien Grill, Florian Strub, Florent Altché, Corentin Tallec, Pierre Richemond, Elena Buchatskaya, Carl Doersch, Bernardo Avila Pires, Zhaohan Guo, Mohammad Gheshlaghi Azar, et al. Bootstrap your own latent-a new approach to self-supervised learning. In *Proceedings of the 33rd Advances in Neural Information Processing System (NIPS)*, volume 33, pp. 21271–21284, 2020.
- Alexandros Haliassos, Konstantinos Vougioukas, Stavros Petridis, and Maja Pantic. Lips don’t lie: A generalisable and robust approach to face forgery detection. In *Proceedings of the 34th IEEE/CVF Conference on Computer Vision and Pattern Recognition (CVPR)*, pp. 5039–5049, 2021.
- Alexandros Haliassos, Rodrigo Mira, Stavros Petridis, and Maja Pantic. Leveraging real talking faces via self-supervision for robust forgery detection. In *Proceedings of the 35th IEEE/CVF Conference on Computer Vision and Pattern Recognition (CVPR)*, pp. 14950–14962, 2022.
- Kaiming He, Xiangyu Zhang, Shaoqing Ren, and Jian Sun. Deep residual learning for image recognition. In *Proceedings of the 29th IEEE/CVF Conference on Computer Vision and Pattern Recognition (CVPR)*, pp. 770–778, 2016.
- Kaiming He, Xinlei Chen, Saining Xie, Yanghao Li, Piotr Dollár, and Ross Girshick. Masked autoencoders are scalable vision learners. *arXiv preprint arXiv:2111.06377*, 2021.
- François Hernandez, Vincent Nguyen, Sahar Ghannay, Natalia A. Tomashenko, and Yannick Estève. TED-LIUM 3: Twice as much data and corpus repartition for experiments on speaker adaptation. In *International Conference on Speech and Computer*, volume 11096, pp. 198–208, 2018.
- Wei-Ning Hsu, Benjamin Bolte, Yao-Hung Hubert Tsai, Kushal Lakhotia, Ruslan Salakhutdinov, and Abdelrahman Mohamed. Hubert: Self-supervised speech representation learning by masked prediction of hidden units. *IEEE/ACM Transactions on Audio, Speech, and Language Processing*, 29:3451–3460, 2021.
- Gao Huang, Yu Sun, Zhuang Liu, Daniel Sedra, and Kilian Q Weinberger. Deep networks with stochastic depth. In *Proceedings of the 14th European Conference on Computer Vision (ECCV)*, pp. 646–661, 2016.
- Sergey Ioffe and Christian Szegedy. Batch normalization: Accelerating deep network training by reducing internal covariate shift. In *Proceedings of the 32nd International Conference on Machine Learning (ICML)*, volume 37 of *JMLR Workshop and Conference Proceedings*, pp. 448–456, 2015.
- Kazuki Irie, Albert Zeyer, Ralf Schlüter, and Hermann Ney. Language modeling with deep transformers. *arXiv preprint arXiv:1905.04226*, 2019.
- Bruno Korbar, Du Tran, and Lorenzo Torresani. Cooperative learning of audio and video models from self-supervised synchronization. *Proceedings of the 31st Advances in Neural Information Processing System (NIPS)*, 31, 2018.
- Taku Kudo and John Richardson. Sentencepiece: A simple and language independent subword tokenizer and detokenizer for neural text processing. In *Proceedings of the 56th Conference of the Association for Computational Linguistics (ACL)*, pp. 66–71, 2018.
- Ilya Loshchilov and Frank Hutter. Sgdr: Stochastic gradient descent with warm restarts. In *Proceedings of the 5th International Conference on Learning Representations (ICLR)*, 2017.
- Ilya Loshchilov and Frank Hutter. Decoupled weight decay regularization. In *Proceedings of the 7th International Conference on Learning Representations (ICLR)*, 2019.

- 
- Pingchuan Ma, Rodrigo Mira, Stavros Petridis, Björn W. Schuller, and Maja Pantic. LiRA: Learning visual speech representations from audio through self-supervision. In *Proceedings of the 22nd Annual Conference of International Speech Communication Association (INTERSPEECH)*, pp. 3011–3015, 2021a.
- Pingchuan Ma, Stavros Petridis, and Maja Pantic. End-to-end audio-visual speech recognition with conformers. In *Proceedings of the 46th IEEE International Conference on Acoustics, Speech and Signal Processing (ICASSP)*, pp. 7613–7617, 2021b.
- Pingchuan Ma, Stavros Petridis, and Maja Pantic. Visual speech recognition for multiple languages in the wild. *arXiv preprint arXiv:2202.13084*, 2022.
- Shuang Ma, Zhaoyang Zeng, Daniel McDuff, and Yale Song. Contrastive learning of global and local audio-visual representations. *arXiv preprint arXiv:2104.05418*, 2021c.
- Takaki Makino, Hank Liao, Yannis Assael, Brendan Shillingford, Basilio Garcia, Otavio Braga, and Olivier Siohan. Recurrent neural network transducer for audio-visual speech recognition. In *Proceedings of the IEEE Automatic Speech Recognition and Understanding (ASRU) Workshop*, pp. 905–912, 2019.
- Brais Martinez, Pingchuan Ma, Stavros Petridis, and Maja Pantic. Lipreading using temporal convolutional networks. In *Proceedings of the 45th IEEE International Conference on Acoustics, Speech and Signal Processing (ICASSP)*, pp. 6319–6323, 2020.
- Rodrigo Mira, Alexandros Haliassos, Stavros Petridis, Björn W Schuller, and Maja Pantic. Svts: Scalable video-to-speech synthesis. *arXiv preprint arXiv:2205.02058*, 2022.
- Abdelrahman Mohamed, Hung-yi Lee, Lasse Borgholt, Jakob D Havtorn, Joakim Edin, Christian Igel, Katrin Kirchhoff, Shang-Wen Li, Karen Livescu, Lars Maaløe, et al. Self-supervised speech representation learning: A review. *arXiv preprint arXiv:2205.10643*, 2022.
- Pedro Morgado, Nuno Vasconcelos, and Ishan Misra. Audio-visual instance discrimination with cross-modal agreement. In *Proceedings of the 34th IEEE/CVF Conference on Computer Vision and Pattern Recognition (CVPR)*, pp. 12475–12486, 2021.
- Arsha Nagrani, Samuel Albanie, and Andrew Zisserman. Learnable pins: Cross-modal embeddings for person identity. In *Proceedings of the 15th European Conference on Computer Vision (ECCV)*, pp. 71–88, 2018a.
- Arsha Nagrani, Samuel Albanie, and Andrew Zisserman. Seeing voices and hearing faces: Cross-modal biometric matching. In *Proceedings of the 31st IEEE/CVF Conference on Computer Vision and Pattern Recognition (CVPR)*, pp. 8427–8436, 2018b.
- Vinod Nair and Geoffrey E Hinton. Rectified linear units improve restricted boltzmann machines. In *Proceedings of the 17th International Conference on Machine Learning (ICML)*, 2010.
- Xichen Pan, Peiyu Chen, Yichen Gong, Helong Zhou, Xinbing Wang, and Zhouhan Lin. Leveraging uni-modal self-supervised learning for multimodal audio-visual speech recognition. In *Proceedings of the 60th Conference of the Association for Computational Linguistics (ACL)*, pp. 4491–4503, 2022.
- Vassil Panayotov, Guoguo Chen, Daniel Povey, and Sanjeev Khudanpur. Librispeech: An ASR corpus based on public domain audio books. In *Proceedings of the 40th IEEE International Conference on Acoustics, Speech and Signal Processing (ICASSP)*, pp. 5206–5210, 2015.
- Mandela Patrick, Yuki M Asano, Polina Kuznetsova, Ruth Fong, Joao F Henriques, Geoffrey Zweig, and Andrea Vedaldi. Multi-modal self-supervision from generalized data transformations. *arXiv preprint arXiv:2003.04298*, 2020.
- Stavros Petridis, Themis Stafylakis, Pingchuan Ma, Georgios Tzimiropoulos, and Maja Pantic. Audio-visual speech recognition with a hybrid ctc/attention architecture. In *2018 IEEE Spoken Language Technology Workshop (SLT)*, pp. 513–520, 2018.

- 
- K. R. Prajwal, Triantafyllos Afouras, and Andrew Zisserman. Sub-word level lip reading with visual attention. In *Proceedings of the 35th IEEE/CVF Conference on Computer Vision and Pattern Recognition*, 2022.
- Alec Radford, Karthik Narasimhan, Tim Salimans, and Ilya Sutskever. Improving language understanding with unsupervised learning. <https://openai.com/blog/language-unsupervised>, 2018. [Online; accessed 28-September-2022].
- Alec Radford, Jeffrey Wu, Rewon Child, David Luan, Dario Amodei, Ilya Sutskever, et al. Language models are unsupervised multitask learners. *OpenAI blog*, 1(8):9, 2019.
- Mirco Ravanelli, Jianyuan Zhong, Santiago Pascual, Pawel Swietojanski, Joao Monteiro, Jan Trmal, and Yoshua Bengio. Multi-task self-supervised learning for robust speech recognition. In *Proceedings of the 45th IEEE International Conference on Acoustics, Speech and Signal Processing (ICASSP)*, pp. 6989–6993, 2020.
- Adria Recasens, Pauline Luc, Jean-Baptiste Alayrac, Luyu Wang, Florian Strub, Corentin Tallec, Mateusz Malinowski, Viorica Pătrăucean, Florent Altché, Michal Valko, et al. Broaden your views for self-supervised video learning. In *Proceedings of the 18th IEEE/CVF International Conference on Computer Vision (ICCV)*, pp. 1255–1265, 2021.
- Sucheng Ren, Yong Du, Jianming Lv, Guoqiang Han, and Shengfeng He. Learning from the master: Distilling cross-modal advanced knowledge for lip reading. In *Proceedings of the 34th IEEE/CVF Conference on Computer Vision and Pattern Recognition (CVPR)*, pp. 13325–13333, 2021.
- Pierre H Richemond, Jean-Bastien Grill, Florent Altché, Corentin Tallec, Florian Strub, Andrew Brock, Samuel Smith, Soham De, Razvan Pascanu, Bilal Piot, et al. Byol works even without batch statistics. *arXiv preprint arXiv:2010.10241*, 2020.
- Antony W Rix, John G Beerends, Michael P Hollier, and Andries P Hekstra. Perceptual evaluation of speech quality (pesq)-a new method for speech quality assessment of telephone networks and codecs. In *2001 IEEE international conference on acoustics, speech, and signal processing. Proceedings (Cat. No. 01CH37221)*, volume 2, pp. 749–752. IEEE, 2001.
- Dmitriy Serdyuk, Otavio Braga, and Olivier Siohan. Audio-visual speech recognition is worth 32x32x8 voxels. In *Proceedings of the IEEE Automatic Speech Recognition and Understanding (ASRU) Workshop*, 2021.
- Dmitriy Serdyuk, Otavio Braga, and Olivier Siohan. Transformer-based video front-ends for audio-visual speech recognition. *CoRR*, abs/2201.10439, 2022.
- Changchong Sheng, Matti Pietikäinen, Qi Tian, and Li Liu. Cross-modal self-supervised learning for lip reading: When contrastive learning meets adversarial training. In *Proceedings of the 29th ACM International Conference on Multimedia*, pp. 2456–2464, 2021.
- Bowen Shi, Wei-Ning Hsu, Kushal Lakhota, and Abdelrahman Mohamed. Learning audio-visual speech representation by masked multimodal cluster prediction. In *Proceedings of the 10th International Conference on Learning Representations (ICLR)*, 2022.
- B. Shillingford, Y. Assael, M. W Hoffman, T. Paine, C. Hughes, U. Prabhu, H. Liao, H. Sak, K. Rao, L. Bennett, et al. Large-scale visual speech recognition. In *Proceedings of the 20th Annual Conference of International Speech Communication Association (INTERSPEECH)*, pp. 4135–4139, 2019.
- Abhinav Shukla, Stavros Petridis, and Maja Pantic. Does visual self-supervision improve learning of speech representations for emotion recognition. *IEEE Transactions on Affective Computing*, pp. 1–1, 2021.
- Cees H Taal, Richard C Hendriks, Richard Heusdens, and Jesper Jensen. An algorithm for intelligibility prediction of time–frequency weighted noisy speech. *IEEE Transactions on Audio, Speech, and Language Processing*, 19(7):2125–2136, 2011.
- Zhan Tong, Yibing Song, Jue Wang, and Limin Wang. Videomae: Masked autoencoders are data-efficient learners for self-supervised video pre-training. *arXiv preprint arXiv:2203.12602*, 2022.

- 
- Hugo Touvron, Matthieu Cord, Alexandre Sablayrolles, Gabriel Synnaeve, and Hervé Jégou. Going deeper with image transformers. In *Proceedings of the 18th IEEE/CVF International Conference on Computer Vision (ICCV)*, pp. 32–42, 2021.
- Ashish Vaswani, Noam Shazeer, Niki Parmar, Jakob Uszkoreit, Llion Jones, Aidan N Gomez, Łukasz Kaiser, and Illia Polosukhin. Attention is all you need. In *Proceedings of the 31st Annual Conference on Neural Information Processing Systems (NIPS)*, pp. 5998–6008, 2017.
- Shinji Watanabe, Takaaki Hori, Suyoun Kim, John R Hershey, and Tomoki Hayashi. Hybrid ctc/attention architecture for end-to-end speech recognition. *IEEE Journal of Selected Topics in Signal Processing*, 11(8):1240–1253, 2017.
- Shinji Watanabe, Takaaki Hori, Shigeki Karita, Tomoki Hayashi, Jiro Nishitoba, Yuya Unno, Nelson Enrique Yalta Soplín, Jahn Heymann, Matthew Wiesner, Nanxin Chen, Adithya Renduchintala, and Tsubasa Ochiai. ESPnet: End-to-end speech processing toolkit. In *Proceedings of the 19th Annual Conference of International Speech Communication Association (INTERSPEECH)*, pp. 2207–2211, 2018.
- Chen Wei, Haoqi Fan, Saining Xie, Chao-Yuan Wu, Alan Yuille, and Christoph Feichtenhofer. Masked feature prediction for self-supervised visual pre-training. *arXiv preprint arXiv:2112.09133*, 2021.
- Zhenda Xie, Zheng Zhang, Yue Cao, Yutong Lin, Jianmin Bao, Zhuliang Yao, Qi Dai, and Han Hu. Simmim: A simple framework for masked image modeling. In *Proceedings of the 35th IEEE/CVF Conference on Computer Vision and Pattern Recognition (CVPR)*, pp. 9653–9663, 2022.
- Bo Xu, Cheng Lu, Yandong Guo, and Jacob Wang. Discriminative multi-modality speech recognition. In *Proceedings of the 33rd IEEE/CVF Conference on Computer Vision and Pattern Recognition (CVPR)*, pp. 14433–14442, 2020.
- Qiantong Xu, Alexei Baevski, Tatiana Likhomanenko, Paden Tomasello, Alexis Conneau, Ronan Collobert, Gabriel Synnaeve, and Michael Auli. Self-training and pre-training are complementary for speech recognition. In *Proceedings of the 46th IEEE International Conference on Acoustics, Speech and Signal Processing (ICASSP)*, pp. 3030–3034, 2021.
- Jianwei Yu, Shi-Xiong Zhang, Jian Wu, Shahram Ghorbani, Bo Wu, Shiyin Kang, Shansong Liu, Xunying Liu, Helen Meng, and Dong Yu. Audio-visual recognition of overlapped speech for the lrs2 dataset. In *Proceedings of the 45th IEEE International Conference on Acoustics, Speech and Signal Processing (ICASSP)*, pp. 6984–6988, 2020.
- Zi-Qiang Zhang, Jie Zhang, Jian-Shu Zhang, Ming-Hui Wu, Xin Fang, and Li-Rong Dai. Learning contextually fused audio-visual representations for audio-visual speech recognition. *arXiv preprint arXiv:2202.07428*, 2022.

---

Hyperparameter	Value
Training epochs	150
Warmup epochs	40 (LRS3), 30 (LRS3+Vox2-en)
Optimiser	AdamW
Learning rate	3e-3 (Base), 2e-3 (Large)
Optimiser ( $\beta_1, \beta_2$ )	(0.9, 0.999)
Weight decay	0.04
Learning rate schedule	Cosine decay
Drop path	0.05 (Base), 0.1 (Large)
Gradient clip	5.0
Video augmentations	RandomCrop + HorizontalFlip

Table 6: **Pre-training settings.**

## A DATASET / IMPLEMENTATION DETAILS

### A.1 DATASETS

**LRS3.** LRS3 (Afouras et al., 2018b) is the largest publicly available transcribed audio-visual dataset for continuous speech recognition. It consists of around 430 hours of spoken sentences from TED talks, with a vocabulary of more than 50,000 words uttered by thousands of speakers. The test set contains around 1 hour of utterances with speakers separate from those in the training set.

**LRS2.** The 223-hour LRS2 dataset (Chung et al., 2017), collected from BBC programmes, is the second-largest publicly available transcribed audio-visual dataset for continuous speech recognition. As LRS3, it contains an unconstrained vocabulary and thousands of diverse speakers.

**VoxCeleb2.** VoxCeleb2 (Chung et al., 2018) is a non-transcribed dataset containing YouTube-downloaded videos. It consists of around 2,500 hours of utterances with over 6,000 speakers. Since VoxCeleb2 is multi-lingual, as mentioned in the main text, we use an English-only version curated by Shi et al. (2022), amounting to 1,759 hours.

### A.2 DATASET PRE-PROCESSING

We follow common practices in the literature for dataset pre-processing (Ma et al., 2022; Shi et al., 2022; Martinez et al., 2020). We use RetinaFace (Deng et al., 2020) to detect the faces and FAN (Bulat & Tzimiropoulos, 2017) to compute 68 facial landmarks for each video frame. We average the landmarks using a moving window of 12 frames to reduce motion jitter, and for each frame we perform affine warping to the mean face using the resulting smoothed landmarks. We crop a  $96 \times 96$  region centred around the mouth and finally transform to grayscale. Raw audio is used without any pre-processing nor normalisation. Utterances longer than 24 seconds are split into smaller constituents.

### A.3 PRE-TRAINING

Table 6 provides the default setting for pre-training. We use the AdamW (Loshchilov & Hutter, 2019) optimiser with linear learning rate warmup (Goyal et al., 2017) and a cosine decay schedule (Loshchilov & Hutter, 2017). During training, we apply random spatial cropping of size  $(88 \times 88)$  followed by horizontal flipping with probability 0.5. These augmentations are applied in a time-consistent manner across the video clips to maintain temporal coherence. We do not use any augmentations for the raw audio. We also use stochastic depth (Huang et al., 2016) for regularisation, as well as LayerScale (Touvron et al., 2021) with coefficient 0.1. We train the Base model with 32 A100 GPUs, and the Large model with 128. It takes around 15 minutes / 1 hour per epoch to pre-train our Base models on LRS3 / LRS3+Vox2-en, and 2 hours per epoch for our Large model on LRS3+Vox2-en.

Hyperparameter	Value
Training epochs	75 (HR), 50 (LR)
Warmup epochs	20
Optimiser	AdamW
Learning rate encoder	2e-3
Learning rate decoder	6e-3
Optimiser $(\beta_1, \beta_2)$	(0.9, 0.98)
Weight decay	0.04 (HR), 0.1 (LR)
Learning rate schedule	Cosine decay
Layer-wise learning rate decay	0.75 (HR), 0.5 (LR)
Minimum learning rate	1e-5
Drop path	0.2
Gradient clip	5.0
Video augmentations	RandomCrop + HorizontalFlip + TimeMask
Audio augmentations	TimeMask
Decoder blocks	6 (Base), 9 (Large)
Decoder hidden size	256 (LR), 512 (HR, Base), 1024 (HR, Large)
Decoder MLP size	1024 (LR), 2048 (HR, Base), 4096 (HR, Large)
Decoder attention heads	4 (LR), 8 (HR, Base), 16 (HR, Large)

Table 7: **Fine-tuning settings.** HR denotes high-resource labelled data setting and LR low-resource.

Our batching process is as follows: The samples are sorted based on their length to minimise zero-padding, and then samples with the same length are randomly shuffled at the beginning of each training epoch. Each batch contains a maximum of 96 / 36 seconds of footage for Base / Large.

#### A.4 FINE-TUNING / DECODING

The protocol for fine-tuning is similar to that for pre-training with some exceptions (see Table 7). We use a higher learning rate for the decoder than for the pre-trained encoder, since the decoder is randomly-initialised. We also employ layer-wise learning rate decay (Clark et al., 2020), which we found to reduce overfitting. In addition to the augmentations from the pre-training stage, we apply time masking (Ma et al., 2022) for both video and audio clips. Specifically, for each second of the sample, we use zero-masking with a duration that is uniformly sampled between 0 and 0.4 seconds. Fine-tuning Base (for both VSR and ASR) takes around 30 seconds per epoch in the low-resource setting and 7 minutes per epoch in the high-resource setting. Fine-tuning Large takes approximately 1 minute and 20 minutes per epoch in the low- and high-resource setting, respectively.

**CTC/attention decoding.** We use joint CTC/attention decoding to map the input sequence  $x$  of length  $T$  to a target sequence  $y = (y_1, \dots, y_L)$  of size  $L$ . The CTC loss during fine-tuning is given by

$$\mathcal{L}_{\text{ctc}} = -\log \sum_{A \in A_{x,y}} \left( \prod_{t=1}^T p_t(a_t|x) \right), \quad (5)$$

where  $A_{x,y}$  is the set of valid alignments,  $A$  is one such alignment, and  $a_t$  is the token at time-step  $t$ .

The attention loss, computed using the Transformer decoder outputs, can be expressed as

$$\mathcal{L}_{\text{att}} = -\sum_{l=1}^L \log p(y_l|y_1, \dots, y_{l-1}, x). \quad (6)$$

The final loss during fine-tuning is given by  $\mathcal{L} = \alpha \mathcal{L}_{\text{ctc}} + (1 - \alpha) \mathcal{L}_{\text{att}}$ , where  $\alpha = 0.1$ .

We use the ESPnet framework (Watanabe et al., 2018) for decoding. We set the beam size to 40. The final score used to choose the most likely sequence is given by  $\mathcal{S} = \lambda \mathcal{S}_{\text{ctc}} + (1 - \lambda) \mathcal{S}_{\text{att}} + \beta \mathcal{S}_{LM}$ , where  $\mathcal{S}_{\text{ctc}}$  and  $\mathcal{S}_{\text{att}}$  denote the scores from the CTC and attention branches, respectively, and  $\lambda = 0.1$ .  $\mathcal{S}_{LM}$

stage	filters	output size
conv <sub>1</sub>	$5 \times 7 \times 7, 64, \text{stride } 1 \times 2 \times 2$	$T \times 44 \times 44$
pool <sub>1</sub>	max, $1 \times 3 \times 3, \text{stride } 1 \times 2 \times 2$	$T \times 22 \times 22$
res <sub>1</sub>	$\begin{bmatrix} 3 \times 3, 64 \\ 3 \times 3, 64 \end{bmatrix} \times 2$	$T \times 22 \times 22$
res <sub>2</sub>	$\begin{bmatrix} 3 \times 3, 128 \\ 3 \times 3, 128 \end{bmatrix} \times 2$	$T \times 11 \times 11$
res <sub>3</sub>	$\begin{bmatrix} 3 \times 3, 256 \\ 3 \times 3, 256 \end{bmatrix} \times 2$	$T \times 6 \times 6$
res <sub>4</sub>	$\begin{bmatrix} 3 \times 3, 512 \\ 3 \times 3, 512 \end{bmatrix} \times 2$	$T \times 3 \times 3$
pool <sub>2</sub>	global spatial average pool	$T \times 1 \times 1$

(a) Visual feature extractor.

stage	filters	output size
conv <sub>1</sub>	80, 64, stride 4	$160T$
res <sub>1</sub>	$\begin{bmatrix} 3, 64 \\ 3, 64 \end{bmatrix} \times 2$	$160T$
res <sub>2</sub>	$\begin{bmatrix} 3, 128 \\ 3, 128 \end{bmatrix} \times 2$	$80T$
res <sub>3</sub>	$\begin{bmatrix} 3, 256 \\ 3, 256 \end{bmatrix} \times 2$	$40T$
res <sub>4</sub>	$\begin{bmatrix} 3, 512 \\ 3, 512 \end{bmatrix} \times 2$	$20T$
pool <sub>2</sub>	average pool, stride 20	$T$

(b) Auditory feature extractor.

Table 8: **Feature extractors.** We provide details on the convolutional architectures used as the feature extractors for the visual and auditory modalities. Note that the output sizes for both networks match.

is an optional score from the language model, incorporated through shallow fusion (Watanabe et al., 2017). When using a language model,  $\beta$  is chosen from  $\{0.1, 0.2, 0.3, 0.4\}$  using the validation set.

Inference on one A100 GPU (without batching) takes around 3 seconds to decode 10 seconds of footage for Base and 5 seconds for Large.

**Language model.** We use a 16-block Transformer-based language model, as proposed by Irie et al. (2019). The hidden size/MLP size/attention heads are 512/2048/8. The language model is trained on the combination of the following datasets: Librispeech (Panayotov et al., 2015), LRS2/3, TED-LIUM 3 (Hernandez et al., 2018), VoxForge and Common Voice (Ardila et al., 2020). The total number of characters is 166 million.

## A.5 FEATURE EXTRACTORS

The details of the visual and auditory convolutional feature extractors are provided in Tables 8a and 8b, respectively.

## B LRS2 EXPERIMENTS

We report results on the test set of the LRS2 dataset (Chung et al., 2017) in Table 9. After pre-training on the LRS3 or the LRS3+Vox2-en datasets, we fine-tune on the “pre-training” and “training” sets of LRS2. We observe similar trends as in the LRS3 experiments (Table 2), namely that performance is benefited from large models, large unlabelled datasets, and self-training. We significantly outperform all other methods, including one (Pan et al., 2022) pre-trained on 60,000 hours of audio data.

## C MORE ABLATIONS

### C.1 MORE PRE-TRAINING ABLATIONS

**Momentum parameter.** Table 10a shows the effect of varying the momentum parameter for updating the teacher networks. We show results at three coarse levels: 0 (teacher is a copy of the student at each iteration), 0.999 (with a cosine schedule to 1), and 1 (teacher does not get updated during training). We see that using a momentum value of 0 leads to representation collapse. At the other extreme, a value of 1 does not allow the teacher targets to improve during training, leading to poor representations. A slowly-evolving momentum encoder is most effective.

Method	Encoder	LM	Unlab hours	Lab hours	WER (%)	
					VSR	ASR
<i>supervised</i>						
Chung et al. (2017)	LSTM	✓	-	223	70.4	-
Petridis et al. (2018)	LSTM	✓	-	380	63.5	8.3
Ren et al. (2021)	Transformer	✗	-	818	49.2	-
Yu et al. (2020)	CNN	✓	-	223	48.9	6.7
Ma et al. (2021b)	Conformer	✓	-	380	37.9	3.9
Prajwal et al. (2022)	Transformer	✓	-	698	28.9	-
Ma et al. (2022)	Conformer	✓	-	818	27.3	-
Prajwal et al. (2022)	Transformer	✓	-	2,676*	<b>22.6</b>	-
<i>semi-supervised (using external models for pseudo-labelling)</i>						
Afouras et al. (2020)	CNN	✓	777	223	51.3	-
Ma et al. (2022)	Conformer	✓	641	818	<b>25.5</b>	-
<i>self-supervised</i>						
Pan et al. (2022)	Transformer	✗	60,000	223	43.2	2.7
Ma et al. (2021a)	Conformer	✓	433	223	38.8	-
RAVEN (Base)	Transformer	✗	433	223	32.1	3.9
RAVEN (Large)	Transformer	✗	1,759	223	24.1	2.8
RAVEN (Large) w/ self-training	Transformer	✗	1,759	223	20.5	<b>2.1</b>
RAVEN (Large) w/ self-training	Transformer	✓	1,759	223	<b>18.6</b>	<b>2.1</b>

Table 9: **LRS2 results.** We report results on the test set with different model sizes and number of unlabelled data hours (Unlab hours). Lab hours denotes the number of labelled hours, and LM denotes whether or not a language model was used during decoding. \*Includes non-publicly available data.

Momentum $\mu$	WER (%)	
	VSR	ASR
0	coll. <sup>‡</sup>	coll. <sup>‡</sup>
0.999 <sup>†</sup>	<b>32.9</b>	<b>12.2</b>
1	75.0	74.0

(a) **Momentum parameter.** It is important for the momentum encoders to slowly evolve during training. <sup>†</sup>Follows a cosine schedule with 0.999 as the starting value. <sup>‡</sup>Denotes representation collapse.

Norm	WER (%)	
	VSR	ASR
BN	<b>32.9</b>	<b>12.2</b>
LN	39.0	12.7

(b) **Pre-MLP normalisation.** Using batchnorm (BN) before the MLPs in the encoder works better than using layernorm (LN).

Table 10: **More pre-training** ablations under the LRS3 low-resource setting using our Base model.

Encoder LR	Decoder LR	WER (%)	
		VSR	ASR
<i>same LR</i>			
$1 \times 10^{-3}$	$1 \times 10^{-3}$	36.1	13.1
$3 \times 10^{-3}$	$3 \times 10^{-3}$	34.0	<b>12.2</b>
$5 \times 10^{-3}$	$5 \times 10^{-3}$	34.8	<b>12.2</b>
<i>different LR</i>			
$1 \times 10^{-3}$	$5 \times 10^{-3}$	<b>32.9</b>	<b>12.2</b>

(a) **Learning rates (LR) for encoder and decoder.** Using a larger learning rate for the decoder than the encoder is beneficial for VSR.

Learning rate decay	WER (%)	
	VSR	ASR
1.0	42.4	12.5
0.75	33.1	<b>11.7</b>
0.50	<b>32.9</b>	12.2
0.25	33.0	12.5

(b) **Learning rate decay.** Reducing the learning rate as the encoder depth decreases improves performance.

Tokens	LM	WER (%)	
		VSR	ASR
Character	✗	35.8	13.6
Character	✓	32.7	11.1
Subword	✗	32.9	12.2
Subword	✓	<b>30.4</b>	<b>10.5</b>

(c) **Tokenisation.** Using subword (SentencePiece) units as targets is better than using characters. A language model (LM) also helps.

Table 11: **Fine-tuning** ablations under the LRS3 low-resource setting using our Base model.

**Pre-MLP normalisation.** As mentioned in the main text, we use batchnorm before each MLP module rather than layernorm, a choice inspired by Chen et al. (2021). Table 10b shows that our method still works with layernorm, but lags behind batchnorm. This is an interesting observation worthy of future exploration. A preliminary hypothesis is that batchnorm may improve the conditioning of the networks at initialisation, leading to better targets at the beginning of training (Richmond et al., 2020).

## C.2 FINE-TUNING ABLATIONS

**Learning rates.** Table 11a studies the effect of using different learning rates for the encoder and decoder. We find that it is beneficial for VSR to use a higher learning rate for the decoder than the encoder, likely because the encoder is pre-trained, whereas the decoder is randomly-initialised and thus requires a larger learning rate to search for a more effective local optimum.

**Learning rate decay.** Table 11b shows the influence of decaying the encoder’s learning rate as the depth of the model decreases. The learning rate at block  $b$ ,  $r_b$ , is given by  $r_b = r_B d^{B-b}$ , where  $B$  is the index of the last block and  $d$  is the learning rate decay (Clark et al., 2020). A decay less than 1 works well for both VSR and ASR, suggesting that during fine-tuning it is useful to employ larger learning rates for the deeper layers, which are more task-specific.

**Tokenisation.** In Table 11c, we compare the use of characters with SentencePiece (Kudo & Richardson, 2018) subword units (vocabulary size of 1,000) as our target tokens. We find that using subword units leads to superior results than character units. This may be explained by the language priors embedded in subword units, which facilitate speech recognition.

## C.3 AUDIO-VISUAL FINE-TUNING

It is possible to use the learned auditory and visual representations for audio-visual speech recognition. To that end, following Ma et al. (2021b), we concatenate the outputs of the two encoders, feed the resulting embeddings to a 2-layer MLP module with hidden size 4096 and batchnorm, and then fine-tune for speech recognition, as described in Section 3.2. We initialise the video and audio

Fine-tune setting	Resource	WER (%)
Audio-only	Low	2.6
Audio-visual	Low	2.5
Audio-only	High	1.4
Audio-visual	High	1.4

Table 12: **Audio vs audio-visual learning on LRS3 test set..** Including the visual modality for fine-tuning has very little influence in clean conditions.

Model	Transcription
Groundtruth	So what do you think happens to these gals
VSR, low-resource, base, LRS3	So what <b>did the thing I would see this talk</b>
VSR, high-resource, large, LRS3+Vox2-en	So what do you think happens <b>this is an accident</b>
ASR, low-resource, base, LRS3	So what do you think happens to these <b>look outs</b>
ASR, high-resource, large, LRS3+Vox2-en	So what do you think happens to these gals
Groundtruth	project really is to find photographs that were taken before something
VSR, low-resource, base, LRS3	<b>projects</b> really <b>has</b> to find photographs <b>on which I can</b> before something
VSR, high-resource, large, LRS3+Vox2-en	<b>process</b> really is to find photographs that were taken before something
ASR, low-resource, base, LRS3	project really is to find photographs that <b>we're taking</b> before something
ASR, high-resource, large, LRS3+Vox2-en	project really is to find photographs that were taken before something
Groundtruth	Why are we embedded in social networks
VSR, low-resource, base, LRS3	Why are we <b>admitted</b> social networks
VSR, high-resource, large, LRS3+Vox2-en	Why are we embedded in social networks
ASR, low-resource, base, LRS3	Why are we <b>in better</b> social networks
ASR, high-resource, large, LRS3+Vox2-en	Why are we embedded in social networks
Groundtruth	They won the game
VSR, low-resource, base, LRS3	<b>Because I wasn't happy</b>
VSR, high-resource, large, LRS3+Vox2-en	<b>They want to come</b>
ASR, low-resource, base, LRS3	They <b>want</b> the game
ASR, high-resource, large, LRS3+Vox2-en	They won the game
Groundtruth	Has it gotten better
VSR, low-resource, base, LRS3	<b>It's not</b> better
VSR, high-resource, large, LRS3+Vox2-en	<b>It's</b> gotten better
ASR, low-resource, base, LRS3	<b>Is</b> it gotten better
ASR, high-resource, large, LRS3+Vox2-en	Has it gotten better

Table 13: **Transcription errors.**

encoders with weights obtained from uni-modal fine-tuning and randomly initialise the rest. We fine-tune for 30 epochs with the hyperparameters used for audio-only fine-tuning, shown in Table 7.

Table 12 shows results in the low- and high-resource settings for the Large model with LRS3+Vox2-en pre-training. Audio-visual training gives marginal improvements (if any) compared to audio-only when the audio is clean (i.e., not noisy), consistent with findings by Ma et al. (2021b). Investigating the impact of audio-visual training and testing on audio corrupted with various noise types, is outside the scope of this work, but is interesting to take up in future work.

## D ANALYSIS OF TRANSCRIPTION ERRORS

We provide examples of transcription errors in Table 13. We consider the Base VSR and ASR models fine-tuned in the low-resource setting (47.0% and 4.7% WER, respectively) and the Large VSR and ASR models fine-tuned in the high-resource setting with self-training and a language model (23.4% and 1.4% WER, respectively). Although the worst model sometimes makes surprising errors (e.g., “They won the game” → “Because I wasn’t happy”), most often the errors are related to words that are phonetically similar (e.g., “were taken” → “we’re taking”, “embedded” → “in better”, “won” → “want”). As expected, the quality of the transcriptions is higher for ASR than VSR, and it improves as we increase the model size and number of unlabelled data points.

---

Method	Encoder	Training dataset	PESQ	STOI	ESTOI
Mira et al. (2022)	Conformer	LRS3	1.25	0.51	0.27
Mira et al. (2022)	Conformer	LRS3+Vox2-en	1.26	0.53	0.31
SVTS from scratch	Transformer	LRS3+Vox2-en	1.26	0.53	0.30
SVTS w/ RAVEn	Transformer	LRS3+Vox2-en	<b>1.30</b>	<b>0.56</b>	<b>0.36</b>

Table 14: **Video-to-speech synthesis on LRS3 test set.** Using RAVEn pre-training for the video encoder provides significant boosts in performance.

## E RAVEN FOR VIDEO-TO-SPEECH SYNTHESIS

We evaluate here whether RAVEn pre-training can benefit tasks other than speech recognition by considering video-to-speech synthesis, which aims to output the speech waveform given the corresponding silent video of lip movements. We follow the protocol of SVTS (Mira et al., 2022), the current state-of-the-art method, to perform video-to-speech on the LRS3 test set after training on LRS3+Vox2-en. We study the effect of initialising the video encoder with the weights from our Large pre-trained model. We use the same hyperparameters as Mira et al. (2022), except that we use a learning rate of  $2e-4$  and train only for 30 epochs (rather than 150). We train the “from scratch” baseline with a learning rate of  $7e-4$  for 50 epochs, as training longer resulted in overfitting.

Table 14 reports performance based on PESQ (Rix et al., 2001), which measures the perceptual quality of the generated samples, as well as STOI and ESTOI (Taal et al., 2011), which measure their intelligibility. The results show that using RAVEn pre-training results in significant improvements in performance, compared with training from scratch, across all metrics. In fact, the performance boosts due to RAVEn pre-training (0.04 / 0.03 / 0.06 for PESQ / STOI / ESTOI) are larger than those observed by Mira et al. (2022) (0.01, 0.02, 0.04) when increasing the training set size by around a factor of 4 (from LRS3 to LRS3+Vox2-en).